Int. J. Solids Structures Vol. 21, No. 2, pp. 145–154, 1985
Printed in the U.S.A.

0020-7683/85 $3.00 + .00
Pergamon Press Ltd.

INSTABILITY OF AN ARTICULATED CANTILEVER INDUCED BY AN IMPINGING AIRJET

Z. L. QIU† AND S. NEMAT-NASSER ‡
Department of Civil Engineering, The Technological Institute, Northwestern University, Evanston, IL 60201, U.S.A.

(*Received* 11 *August* 1983)

Abstract—Experimental results on instability modes of an articulated cantilever, subjected at its free end to an impinging airjet, are presented and compared with linearized numerical estimates. It is reconfirmed that when the surface upon which the airjet impinges is smooth, then the loss of stability occurs by buckling, whereas, with certain metal mesh and sandpaper backing placed on this surface, the loss of stability is by flutter (oscillations with increasing amplitude). With direct and careful measurement of the applied resultant loads, good correlation between the numerical estimates and the experimental results is obtained.

1. INTRODUCTION

In view of their application in aerospace technology, mechanical systems subjected to nonconservative loads received considerable attention in the early and mid 1960s; see, for example, Bolotin [1], Herrmann [2], Herrmann and Bungay [3], Leipholz [4], Nemat-Nasser [5] and Ziegler [6–8]. Most of these efforts were theoretical, and only a few, often qualitative, experimental investigations were made. In particular, a series of mechanical models was developed by Herrmann, Nemat-Nasser and Prasad [9] to illustrate the effect of nonconservative loads on dynamic response and stability of structural elements. This led to one rather extensive quantitative experiment on a two-degrees-of-freedom articulated cantilever subjected at the free end to a nonconservative force produced by an impinging airjet; see Feldt *et al.* [10]. While efforts were made to carefully measure the system parameters, the resultant force on the system had to be measured separately, and this introduced some error, especially in estimation of the critical buckling load.

The purpose of the present paper is to report the results of a new series of experiments on essentially the same system, but with direct measurement of the applied forces and the angular displacements during the entire experiment.

Figures 1, 2 and 3, respectively, show the photograph of the model, a schematic representation of the model and the end attachment upon which an airjet impinges. The attachment is designed for direct measurement of normal and tangential loads. With strain gauges attached appropriately at joints A and B in Fig. 2, relative angular rotations may be measured directly. Therefore, the experiment permits direct verification of the critical flutter and buckling loads. In this experiment, three different systems were tested, where the differences between systems were due to changes in the elastic stiffness associated with each degree of freedom. Rather good correlation between the theoretical prediction and experimental observation is obtained for both buckling- and flutter-type instabilities.

2. DESCRIPTION OF MODEL

The model consists of two like light aluminum rods, R_1 and R_2, an attachment C at the free end, and a nozzle, N, as shown in Fig. 2. Rod R_1 is elastically hinged to the fixed base, B_1, at joint A, while rod R_2 is elastically hinged to R_1 at B. The springs S_2 and S_4 are used to alter the stiffness of the system, as well as to provide a means for

† Permanent address: Associate Professor, Department of Civil Engineering, Qinghua University, Beijing, China.
‡ Professor of Civil Engineering and Applied Mathematics.

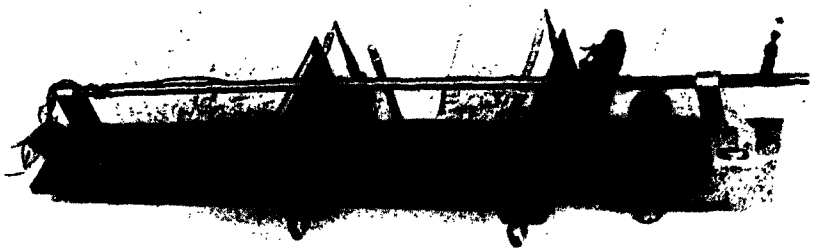

Fig. 1. Photograph of the model.

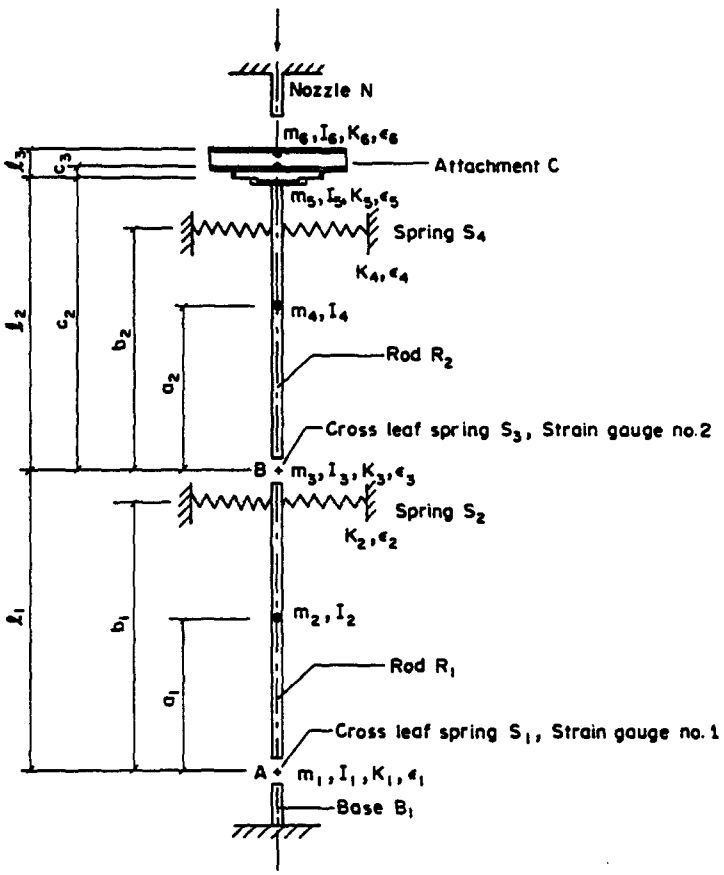

Fig. 2. Schematic of the model.

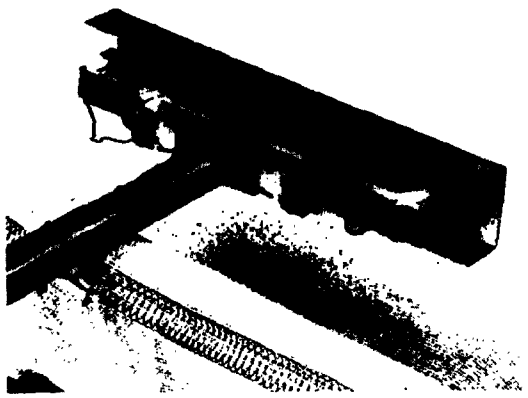

Fig. 3. Photograph of attachment C.

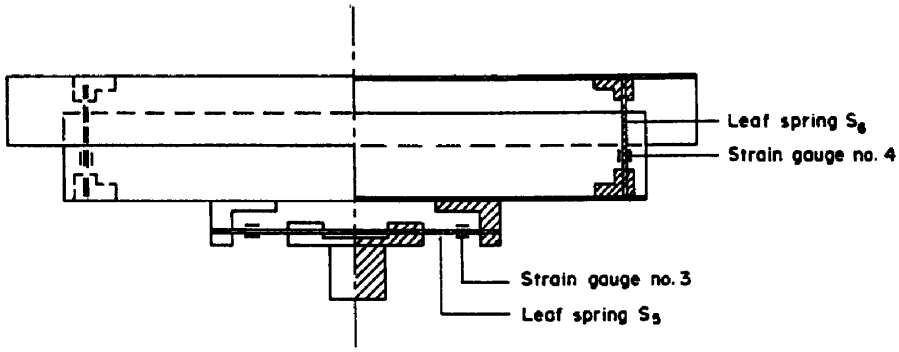

Fig. 4. Schematic of attachment C.

initial alignment. The entire system moves in a horizontal plane, being suspended from the ceiling by long light wires. Hinges A and B consist of cross-leaf springs on which strain gauges, No. 1 and No. 2, are attached for direct measurement of relative angular rotation.

The schematic of attachment C is shown in Fig. 4. It consists of two aluminum channels and two sets of leaf springs; see also Fig. 3. The normal pressure is measured by the set of strain gauges No. 3 attached to leaf springs S_5, and the tangential force is measured by the set of strain gauges No. 4 attached to leaf springs S_6. There are two sets of strain gauges and leaf springs symmetrically placed in order to compensate for asymmetry during measurement.

The airjet through the nozzle N impinges on the face of attachment C. A combination of a metal screen of a certain mesh size and sandpaper backing serves to control the

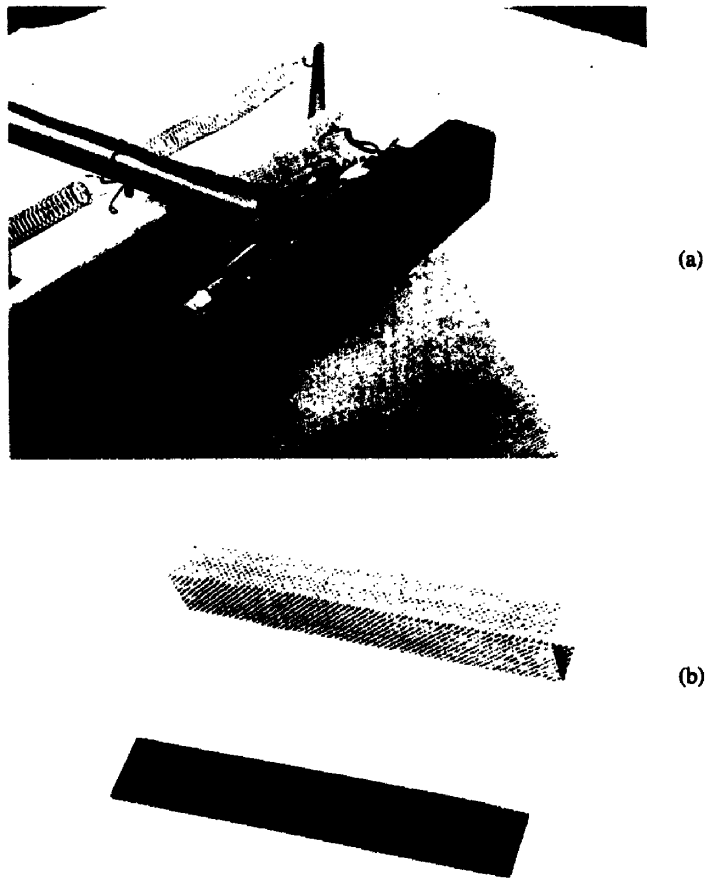

Fig. 5. (a) Attachment with screen; (b) Metal mesh and sandpaper.

orientation of the resultant force, relative to the normal of the attachment face. As has been shown by Nemat-Nasser [11], a system of this kind is adjoint to a system with a follower force. When the resultant force whose point of action always remains along the initial system axis, acts perpendicularly to the attachment face, then the system would be conservative, being the adjoint of the system under dead load. On the other hand, when the orientation of this resultant force varies as a function of the angular rotation of the attachment face, then the system would include nonconservative loads. The limiting case, where the resultant force remains always coaxial with the direction of the impinging jet, is a purely nonconservative load, and the corresponding system is the adjoint of Beck's problem; see Bolotin [1], Herrmann *et al.* [9], Leipholz [12], and Ziegler [6, 7]. The suitable choice of metal mesh and sandpaper backing permits a control on the nature of the applied load. A combination of metal mesh and sandpaper used in the experiments is shown in Fig. 5.

When the attachment face is smooth, the resultant force remains essentially normal to it. The system then buckles at a critical load produced by a critical velocity of the impinging jet. On the other hand, with suitable metal mesh and sandpaper, the system may be made to lose stability by flutter, i.e. oscillation about the straight axis with exponentially increasing amplitude.

The fixed nozzle N provides an airjet, and is aligned along the initial horizontal equilibrium axis of the system.

During the experiment, the greater part of the model is shielded from the air disturbances that the airjet produces, in an effort to minimize the concomitantly induced small amplitude random vibration of the system. The shielding does not interfere with the free motion of the system.

3. SYSTEM PARAMETER ESTIMATES

There are four major elastic spring constants, K_1, K_2, K_3 and K_4 (Fig. 2). These are determined experimentally by static and dynamic methods in a similar manner as discussed by Feldt *et al.* [10]. The static method appears to yield more reliable results than the dynamic one, as for several different tests it shows smaller scatter. Thus, the result of the static method is used in calculating the critical load.

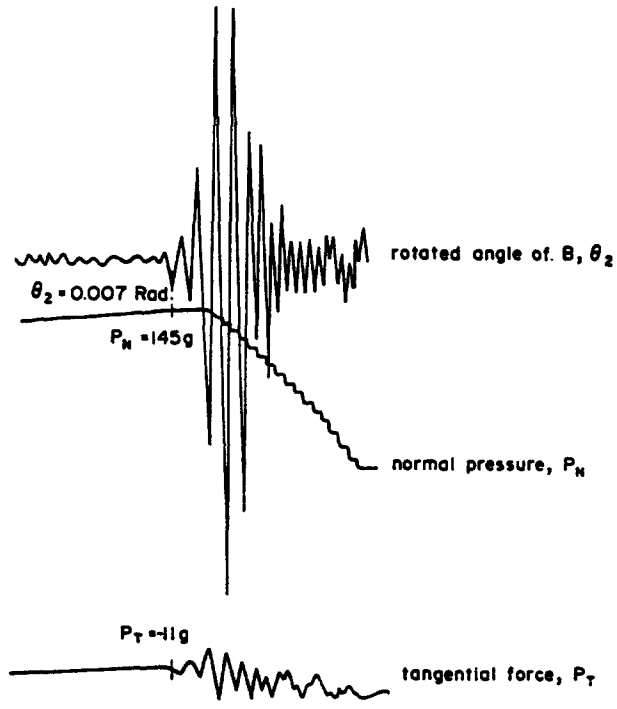

Fig. 6. Records of normal pressure, P_N, tangential force, P_T, and the angular rotation, θ_2, at B.

Table 1. System data

Dimension (cm)	Mass (g s²/cm)	Moment of Inertia (g s² cm)	Damping
$a_1 = 16.6$	$m_1 = 0$†	$I_1 = 0$†	$\epsilon_1 = 2.5$
$a_2 = 16.3$	$m_2 = 3.69 \times 10^{-2}$	$I_2 = 5.021$	$\epsilon_2 = 0$
$c_2 = 32.3$	$m_3 = 0$†	$I_3 = 0$†	$\epsilon_3 = 2.5$
$c_3 = 1.1$	$m_4 = 3.60 \times 10^{-2}$	$I_4 = 4.857$	$\epsilon_4 = 0$
$l_1 = 33.2$	$m_5 = 2.07 \times 10^{-2}$	$I_5 = 0.366$	$\epsilon_5 = 0$
$l_2 = 33.4$	$m_6 = 2.34 \times 10^{-2}$‡	$I_6 = 0.556$‡	$\epsilon_6 = 0$
$l_3 = 2.1$‡	$= 4.82 \times 10^{-2}$§	$= 1.045$§	$\epsilon_7 = 0.003$
$= 2.19$§			

† m_1, I_1, m_3, I_3 are included in m_2, I_2, m_4, I_4 for simplicity.
‡ These data are for buckling.
§ These data include screen and sandpaper for flutter.

	System I	System II	System III
K_1	2740.5	2740.5	2740.5
K_2	0	2.2	2.2
K_3	2213.1	2213.1	2213.1
K_4	2.64	2.64	2.64
K_5	7.05×10^8	7.05×10^8	7.05×10^8
K_6	7414	7414	7414
b_1	—	22.1	30.4
b_2	11.4	11.4	25.4

K_1, K_3, K_5, K_6—g cm/Rad; K_2, K_4—g/cm; b_1, b_2—cm.

There are two other elastic spring constants, K_5 and K_6, associated with attachment C. Since the effect of the flexibility of the attachment C on the basic results is very small, very accurate estimates of these constants are not essential. Therefore, these constants are estimated from the dimensions and the material parameters of the springs.

The critical conditions are defined in the following manner:

(i) For buckling, as the airjet pressure is increased, the displacement of the middle hinge B is monitored. Close to the critical load, this displacement increases considerably, and when it reaches 2.5 cm, the pressure and the resultant forces on attachment C are read and used as the critical values.

Table 2. Summary of numerical results

		Experimental		Theoretical			Error
Run No.	α	*	$P_{CRT.}$ (g)	Undamped flutter (g)	Damped flutter (g)	Buckling (g)	(%)
System I							
1	0.20	*F*	140		135		+4.5
2	0.28	*F*	145		142		+2.1
3	0.29	*F*	145		143		+1.4
4	0.30	*F*	148		144		+2.8
5	0.31	*F*	150		145		+3.4
6	0.32	*F*	140		146		−4.1
7	0.33	*F*	140		148		−5.4
8	0.33	*F*	148		148		0
9	2.00	*B*	150			159	−5.7
10	2.10	*B*	147			158	−7.0
11	2.17	*B*	150			158	−5.1
12	2.23	*B*	145			157	−7.6
13	2.37	*B*	150			157	−4.5
14	2.45	*B*	148			157	−5.7
15	2.80	*B*	150			155	−3.2
16	3.20	*B*	150			154	−2.6

cont

Table 2. (*Continued*)

Run No.	α	Experimental *	Experimental $P_{CRT.}$ (g)	Theoretical Undamped flutter (g)	Theoretical Damped flutter (g)	Theoretical Buckling (g)	Error (%)
System II							
1	0	*F*	140		133		+5.3
2	0.21	*F*	175	164			+6.7
3	0.27	*F*	160	168			−4.8
4	0.28	*F*	155		150		+3.3
5	0.32	*F*	160		152		+5.3
6	0.37	*F*	149		159		−6.3
7	0.39	*F*	160		163		−1.8
8	2.00	*B*	168			175	−4.0
9	2.00	*B*	170			175	−2.9
10	2.19	*B*	170			174	−2.3
11	2.20	*B*	166			174	−4.6
12	2.20	*B*	170			174	−2.3
13	2.26	*B*	165			174	−5.2
System III							
1	2.28	*B*	166			177	−6.2
2	2.40	*B*	166			176	−5.7
3	2.40	*B*	166			176	−5.7
4	2.40	*B*	161			176	−8.5
5	2.45	*B*	156			176	−11.4
6	2.50	*B*	156			175	−10.9
7	2.60	*B*	161			174	−7.5
8	2.60	*B*	156			174	−10.3
9	2.75	*B*	161			173	−6.9

(ii) For flutter, the displacement of joint *B* and the amplitude of the vibration of the system remain very small, until the critical state is approached. Then the system begins to oscillate about its straight equilibrium configuration with increasing amplitude. The variation of the rotation of joint *B* is directly measured (see Fig. 6), and at the inception of this kind of vibration, the resultant loads on attachment *C* are defined as the critical ones.

Table 1 gives the values of the parameters in the model for three different systems. These systems differ from each other because of the change in the location of springs S_2 and S_4. Table 2 summarizes the experimental results and compares them with the theoretical estimates. Note that *g* stands for "gram force," i.e. 980 dynes. Hence, in Table 1, the unit of mass is 980 "gram mass."

4. ANALYSIS AND NUMERICAL RESULTS

The system has a total of four degrees of freedom, two associated with rods R_1 and R_2, and two associated with attachment *C*. The applied external force (induced by the airjet) is assumed to act at the angle $\alpha\phi_3$ with respect to the initial system axis. Therefore, α identifies the degree of nonconservative character of the load. Figure 7 shows the system in a slightly deformed position. The system includes six major constituents. The masses, moments of inertia, the stiffnesses, and the corresponding damping coefficients of these constituents are denoted by m_1–m_6, I_1–I_6, K_1–K_6 and ϵ_1–ϵ_6, respectively. The damping associated with the air flow over the surface of attachment *C* is characterized by coefficient ϵ_7. Note that the two degrees of freedom associated with attachment *C* may be neglected without introducing noticeable errors, because this attachment is very stiff compared with the stiffness of the other two degrees of freedom. The numerical results, however, were obtained by considering all four degrees of freedom.

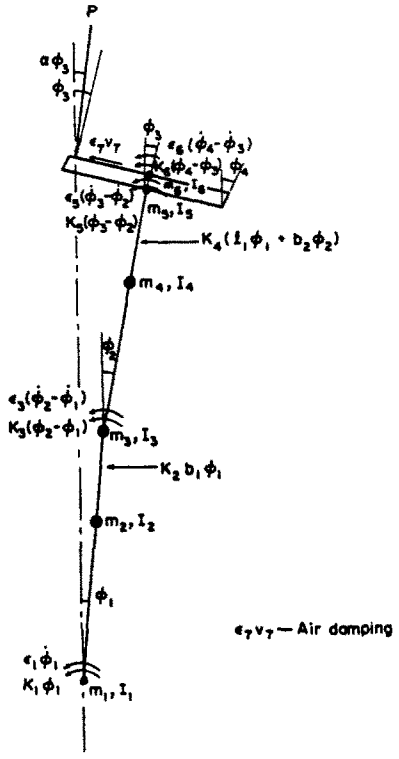

Fig. 7. Schematic of active forces.

The linearized equations of motion are obtained from Lagrange's equation. In the matrix form,

$$[A]\{\ddot{\phi}\} + [B]\{\dot{\phi}\} + [C]\{\phi\} + [R]\{\phi\} = 0 \tag{1}$$

where

$$A_{11} = I_1 + I_2 + a_1^2 m_2 + l_1^2(m_3 + m_4 + m_5 + m_6)$$

$$A_{12} = A_{21} = l_1[a_2 m_4 + c_2(m_5 + m_6)]$$

$$A_{13} = A_{31} = l_1 c_3(m_5 + m_6)$$

$$A_{14} = A_{41} = l_1 l_3 m_6$$

$$A_{22} = I_3 + I_4 + a_2^2 m_4 + c_2^2(m_5 + m_6)$$

$$A_{23} = A_{32} = c_2 c_3(m_5 + m_6)$$

$$A_{24} = A_{42} = c_2 l_3 m_6$$

$$A_{33} = I_5 + I_6 + c_3^2(m_5 + m_6)$$

$$A_{34} = A_{43} = c_3 l_3 m_6$$

$$A_{44} = l_3^2 m_6,$$

$$B_{11} = \epsilon_1 + b_1^2\epsilon_2 + \epsilon_3 + l_1^2\epsilon_4 + l_1^2\epsilon_7$$

$$B_{12} = B_{21} = -\epsilon_3 + l_1 b_2\epsilon_4 + l_1 c_2\epsilon_7$$

$$B_{13} = B_{31} = l_1 c_3\epsilon_7$$

$$B_{14} = B_{41} = l_1 l_3\epsilon_7$$

$$B_{22} = \epsilon_3 + b_2^2\epsilon_4 + \epsilon_5 + c_2^2\epsilon_7$$

$$B_{23} = B_{32} = -\epsilon_5 + c_2 c_3\epsilon_7$$

$$B_{24} = B_{42} = l_3 c_2 \epsilon_7$$

$$B_{33} = \epsilon_5 + \epsilon_6 + c_3^2 \epsilon_7$$

$$B_{34} = B_{43} = -\epsilon_6 + l_3 c_3 \epsilon_7$$

$$B_{44} = \epsilon_6 + l_3^2 \epsilon_7,$$

$$C_{11} = K_1 + b_1^2 K_2 + K_3 + l_1^2 K_4$$

$$C_{12} = C_{21} = -K_3 + l_1 b_2 K_4$$

$$C_{13} = C_{31} = 0$$

$$C_{14} = C_{41} = 0$$

$$C_{22} = K_3 + b_2^2 K_4 + K_5$$

$$C_{23} = C_{32} = -K_5$$

$$C_{24} = C_{42} = 0$$

$$C_{33} = K_5 + K_6$$

$$C_{34} = C_{43} = -K_6$$

$$C_{44} = K_6,$$

$$R_{11} = -Pl_1 \qquad R_{12} = 0$$

$$R_{13} = Pl_1 \alpha \qquad R_{14} = 0$$

$$R_{21} = 0 \qquad R_{22} = -Pc_2$$

$$R_{23} = Pc_2 \alpha \qquad R_{24} = 0$$

$$R_{31} = Pl_1 \qquad R_{32} = Pc_2$$

$$R_{33} = -P[(1 - \alpha)(c_3 + l_3) - c_3] \qquad R_{34} = Pl_3$$

$$R_{41} = 0 \qquad R_{42} = 0$$

$$R_{43} = -Pl_3(1 - \alpha) \qquad R_{44} = 0,$$

are components of matrices $[A]$, $[B]$, $[C]$ and $[R]$, respectively.

Consider the solution,

$$\phi_j(t) = \Phi_j e^{\lambda_j t}, \tag{2}$$

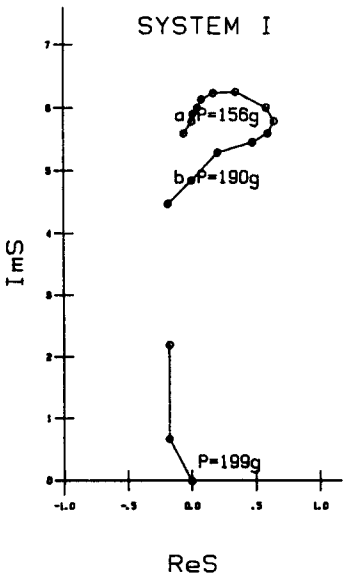

Fig. 8. Eigenvalues in the complex plane; $\alpha = 0.36$, $\epsilon = 2.5$.

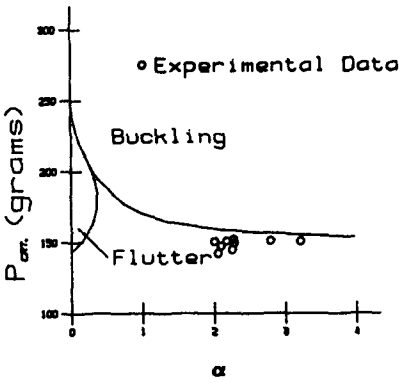

Fig. 9. Stability diagram—System I.

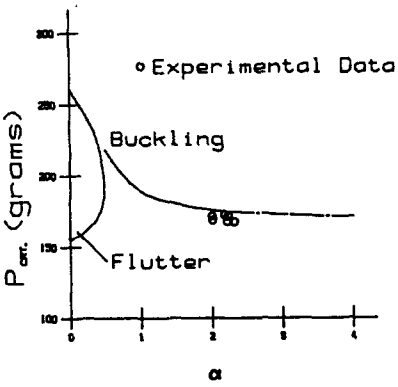

Fig. 10. Stability diagram—System II.

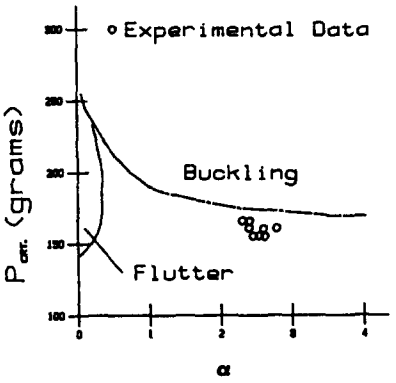

Fig. 11. Stability diagram—System III.

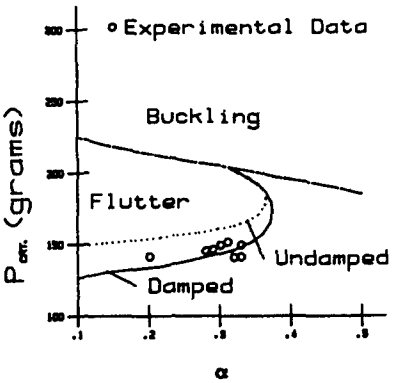

Fig. 12. Stability diagram—System I.

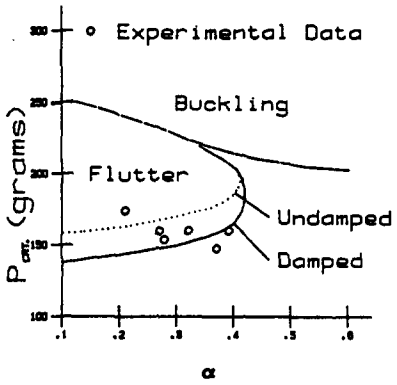

Fig. 13. Stability diagram—System II.

and observe that, if the eigenvalues λ_j have negative real parts, the solution will damp exponentially, whereas it will grow exponentially, if the real part of λ_j is positive. Let S be a typical eigenvalue. The variation of S for System I is shown in Fig. 8. At point 'a' this eigenvalue crosses the imaginary axis from left to right and, therefore, P = 156 g is the critical flutter load. If the crossing occurs at the origin, then we have buckling. For System I in Fig. 8 this occurs at a larger value of P and, therefore, this system flutters first. But, if the flutter is inhibited and the load is increased beyond the buckling value of 199 g, then the loss of stability would be by buckling.

Figures 9–13 give the numerical calculation results, together with the corresponding experimental data. The correlation is rather good and the errors are well within expected limits (see Table 2).

While better accuracy in estimating the buckling load is obtained here, compared with data reported by Feldt *et al.* [10], still lower buckling loads are observed exper-

imentally. Feldt *et al.* present some analysis on the effect of possible imperfections. They show that although the system is not imperfection sensitive, the critical buckling load does reduce in the presence of imperfections, when nonlinear terms are included. This may account for part of the observed discrepancy in the present investigation. Indeed, some initial angular displacement does exist in the system, and the system continues to deform with increasing airjet pressure by a very small amount. This becomes rather large close to the critical state which is arbitrarily defined by a lateral displacement of 2.5 cm for joint B. In view of this, it may be concluded that good correlation between experimental and theoretical results is obtained for buckling type instability.

In the case of flutter, small damping reduces the estimated critical load; see Nemat-Nasser and Herrmann [13]. Figures 12 and 13 show this. The damping parameters had to be estimated (see Table 1). Nevertheless, good correlation between experimental and theoretical results is observed.

REFERENCES

1. V. V. Bolotin, *Nonconservative Problems of the Theory of Elastic Stability*, Moscow (1961); English translation published by Pergamon Press, New York (1963).
2. G. Herrmann, Stability of equilibrium of elastic systems subjected to nonconservative forces. *Appl. Mech. Rev.* **20**, 103–108 (1967).
3. G. Herrmann and R. W. Bungay, On the stability of elastic systems subjected to nonconservative forces. *J. appl. Mech.* **31**, 435–440 (1964).
4. H. Leipholz, Anwendung des Galerkinschen Verfahrens auf nichtkonservative Stabilitätsprobleme des elastischen Stabes. *Z. für angew. Math. Phys.* **13**, 359–372 (1962).
5. S. Nemat-Nasser, Thermoelastic stability under general loads. *Appl. Mech. Rev.* **23**, 615–624 (1970).
6. H. Ziegler, Linear elastic stability. *Z. für angew. Math. Phys.* **4**, 89–184 (1953).
7. H. Ziegler, On the concept of elastic stability. *Advances in Applied Mechanics* (Edited by H. L. Dryden and T. von Karman), Vol. 4, pp. 351–403. Academic Press, New York (1956).
8. H. Ziegler, *Principles of Structural Stability*. Blaisdell, Waltham, MA (1968).
9. G. Herrmann, S. Nemat-Nasser and S. N. Prasad, Models demonstrating instability of nonconservative mechanical systems. Northwestern University Structural Mechanics Laboratory Technical Report No. 66-4 (June 1966).
10. W. T. Feldt, S. Nemat-Nasser, S. N. Prasad and G. Herrmann, Instability of a mechanical system induced by an impinging fluid jet. *J. appl. Mech.* **36**, 693–701 (1969).
11. S. Nemat-Nasser, On circulatory force fields and their adjoints. *J. appl. Mech.* **35**, 829–831 (1968).
12. H. Leipholz, *Stability Theory*. Academic Press, New York (1970).
13. S. Nemat-Nasser and G. Herrmann, Some general considerations concerning the destabilizing effect in nonconservative systems. *J. appl. Math. Phys.* **17**, 305–313 (1966).